Reaction Kinetics and Mechanism for the Gas- and Liquid-Phase Esterification of Acetic Acid with Methanol on Tungstated Zirconia

ARTICLE *in* INDUSTRIAL & ENGINEERING CHEMISTRY RESEARCH · APRIL 2008

Impact Factor: 2.59 · DOI: 10.1021/ie070665a

4 AUTHORS, INCLUDING:

David A Bruce
Clemson University
60 PUBLICATIONS **2,119** CITATIONS

SEE PROFILE

Reaction Kinetics and Mechanism for the Gas- and Liquid-Phase Esterification of Acetic Acid with Methanol on Tungstated Zirconia

Dora E. López, Kaewta Suwannakarn, James G. Goodwin, Jr.,* and David A. Bruce

Department of Chemical and Biomolecular Engineering, Clemson University, Clemson, South Carolina 29634

A comprehensive kinetic investigation of the esterification of acetic acid with methanol in both the liquid phase (21−60 °C) and the gas phase (100−140 °C) was carried out using tungstated zirconia (WZ) as the catalyst. The goal of this study was to derive rate law expressions and to propose a reaction mechanism that would support reaction rate data for esterification on WZ. Upon increasing the concentration of acetic acid, an increase in the rate of esterification was obtained at all reaction temperatures. In contrast, the reaction order with respect to methanol evolved from positive to negative as the reaction temperature increased. Using a model discrimination procedure, we found that a single-site (Eley−Rideal) mechanism with the adsorbed carboxylic acid reacting with the methanol from the gas/liquid phase successfully describes these reactions. One important conclusion of this study was that, even though there were significant differences in the power law exponents for gas- and liquid-phase esterifications, the same reaction mechanism can successfully describe both situations. We propose that the adsorption of the carboxylic acid becomes the rate-determining step (RDS) as the reaction temperature increases. At lower esterification temperatures (liquid phase), the rate-determining step appears to be the nucleophilic attack of the alcohol on the adsorbed/protonated acetic acid molecules. At higher reaction temperature (gas phase), the adsorption of the carboxylic acid becomes rate determining. It was also found that the catalytic activity of WZ was inhibited by water similarly to other strong acid catalysts.

1. Introduction

Esterification reactions are of great industrial importance. A recent significant application for this type of reaction has been in the preparation of biodiesel from "lower quality feedstocks", such as yellow greases, rendered animal fats, and trap greases that contain a significant concentration of free fatty acids (carboxylic acids). Such low-cost feedstocks can be utilized for biodiesel production provided an upstream esterification process is used to convert most of the carboxylic acids into biodiesel esters. This esterification reaction routinely employs strong homogeneous acids (e.g., H_2SO_4) as catalysts,[1] which necessitates that additional separation and neutralization processes be carried out before subsequent base-catalyzed transesterification processes. Therefore, environmental and process economic factors favor the utilization of easily isolated solid acid catalysts for the esterification reactions.[2−4]

To date, many investigations have addressed esterification reactions using homogeneous and heterogeneous acid catalysts.[2−26] For homogeneous-catalyzed esterification reactions, it is generally accepted that the reaction is initiated by the protonation of the carbonyl oxygen of the carboxylic acid, followed by the nucleophilic attack of an alcohol and subsequent decomposition of the intermediate complex species.[2] For solid acid catalysts, several studies have examined whether the carboxylic acid, methanol, or both reactants need to adsorb on the catalyst surface for reaction to occur.[12,13,15,17,24−26] For instance, Altiokka and Çitak[24] suggested that esterification on Amberlite occurs between a protonated isobutanol molecule and acetic acid from the bulk phase. However, most authors agree that the esterification reaction on solid acids is best described by a single-site mechanism, where the carboxylic acid first adsorbs on the catalytic site, followed by reaction with the alcohol from the bulk phase.[12,13,20,25,26] Koster et al.[13] used labeled reactants to demonstrate that gas-phase esterification (125−200 °C) on MCM-type catalysts proceeds through protonated acetic acid ($CH_3COOH_2^+$) not via protonated ethanol ($CH_3CH_2OH_2^+$). Kirumakki et al.[12] studied the liquid-phase esterification of acetic acid with C_3 and C_4 alcohols over different zeolites (Hβ, HY, and HZSM5) at 110−130 °C. Their kinetic data also suggested that esterification follows an Eley−Rideal (ER) pathway, where the alcohol reacts with the adsorbed acetic acid. Likewise, Nijhuis et al.[25] found that an ER model was a better fit than a dual-site model for the liquid-phase esterification of hexanoic acid with 1-octanol on silica-supported Nafion (SAC-13). An ER model has also been found in our laboratory to successfully predict the liquid-phase esterification of acetic acid with methanol on SAC-13.[26] In that study, as the Brønsted acid sites (−SO_3H moieties) were selectively poisoned with pyridine,

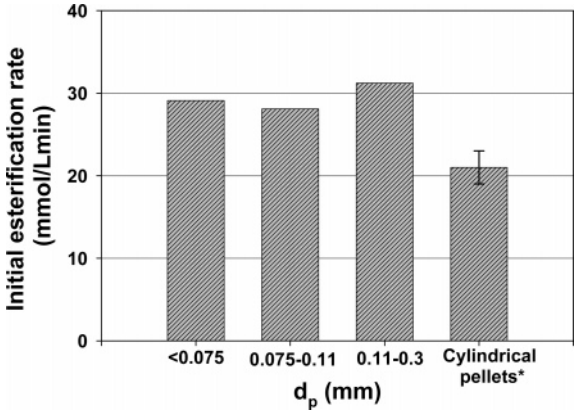

Figure 1. Effect of catalyst particle size on the initial esterification rate of acetic acid with methanol at 60 ± 1 °C [cylindrical pellet size: length = 4.30 ± 0.58 mm, diameter = 2.58 ± 0.09 mm (size estimated using a randomly selected 25-pellet sample)].

* Corresponding author. Fax: (864) 656-0784. Tel.: (864) 656-6614. E-mail: james.goodwin@ces.clemson.edu.

10.1021/ie070665a CCC: $40.75
Published on Web 03/06/2008

Table 1. Initial Autocatalyzed Reaction Rate Data for the Liquid-Phase Esterification of Acetic Acid and Methanol Obtained in the Absence of the Solid Catalyst at Different Reaction Temperatures ($C_{HAc,0}$ = 7.3 M and $C_{MeOH,0}$ = 14.6 M)

T (°C)	$r_0 \times 10^3$ [a] (mol L^{-1} min^{-1})	$k_{auto} \times 10^6$ [b] (L^2 mol^{-1} min^{-1})
21	0.76	0.97
32	1.68	2.15
42	3.03	3.87
52	5.30	6.77
55	6.83	8.73
60	10.7	13.7

[a] Maximum error of the measurement ± 5%. [b] Values obtained using eq 2; maximum error of the estimation ± 9%.

a linear decrease in the initial esterification rate was observed, suggesting that the rate-determining step involved only one site. Although methanol appears to react from the fluid phase via an ER mechanism, it also can adsorb directly on the active sites, but the protonated nucleophile would appear to be unable to carry out the esterification reaction.[26]

In this study, the esterification of a model carboxylic acid with methanol was investigated in order to gain more insight into the kinetics and mechanism of this reaction, important in biodiesel synthesis, on tungstated zirconia (WZ). Supported tungsten oxide catalysts are attracting much attention for esterification and transesterification because of their high acid site strength, mesoporous structure, and thermal stability.[21,23,27−31] These catalytic materials have been shown to efficiently catalyze the esterification of carboxylic acids, such as acetic,[28,31] *n*-octanoic,[21,27] and palmitic[23,30] acid with low-molecular-weight alcohols. Acetic acid (CH_3COOH) is ideal as a model compound for a wide-ranging study of esterification since it has a moderate boiling point (bp 118 °C), can be obtained in pure form, is totally miscible with methanol, and has a concentration that is easily measured by standard analytical techniques (e.g., GC). Structure−reactivity relationships can be used to estimate the esterification reaction rate for larger carboxylic acids, which is known to decrease with increasing hydrocarbon chain length.[20,32−38] This work represents a comprehensive kinetic study of esterification from 21 to 140 °C and from the liquid phase to the gas phase.

2. Experimental Section

Commercially available tungstated zirconia amorphous hydroxide precursor, XZO1251 (16 wt % WO_3, +140 mesh) was donated by Magnesium Electron, Inc. (MEI, Manchester, U.K.). The precursor (XZO1251) was dehydrated at 120 °C for 1 h followed by activation at 700 °C for 2−3 h under air (moisture-free). This calcined catalyst hereinafter will be referred to as WZ700. Catalyst total surface area, total Barrett−Joyner−Halenda (BJH) pore volume, and average pore size were determined using nitrogen isotherms (−196 °C) in a Micromeritic ASAP 2020. Tungsten elemental analysis of WZ700 was carried out using inductively coupled plasma emission spectroscopy (Galbraith Laboratory, Knoxville, TN). The acid site density was determined using an ion-exchange/titration method, whereby WZ700 H^+ ions were exchanged with Na^+ ions followed by titration of the aqueous solution with NaOH (0.05 N).[39]

In order to study the effect of particle size, the activated precursor (XZO1251) calcined at 600 °C (SGN_WZ600) in pellet form (Saint-Gobain NorPro, Stow, OH) was utilized. The pellets utilized were cylindrical shaped, with length = 4.30 mm and diameter = 2.6 mm. The cylindrical pellets were ground using a porcelain mortar and pestle. The ground catalyst was sieved to obtain different ranges of particle sizes: <0.075 mm (+200 mesh), 0.075−0.108 mm (200−140 mesh), and 0.108−0.30 mm (140−50 mesh). The sieved fractions were calcined using the procedure outlined above (same as WZ700) to obtain a more active material (discussed later).

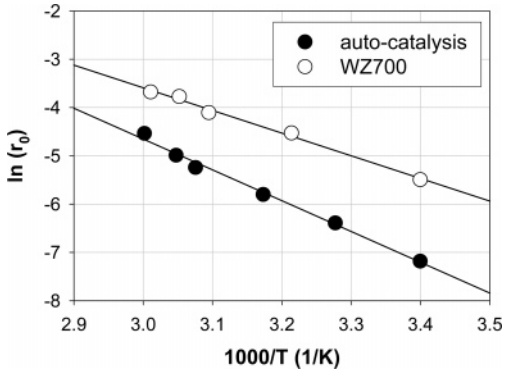

Figure 2. Arrhenius plots for the liquid-phase esterification of acetic acid with methanol using CH_3COOH (autocatalysis) and WZ700 (C_{cat} = 60 g/L) as catalyst in the 21−60 °C temperature range (initial reaction rate, r_0, in mol L^{-1} min^{-1}).

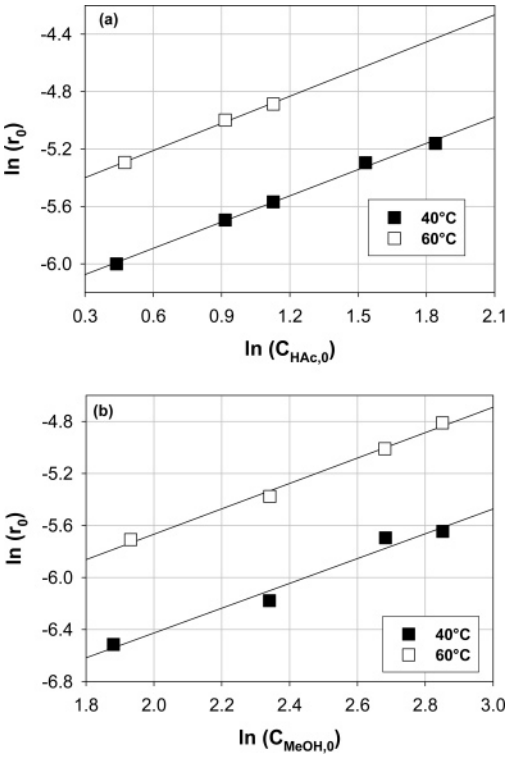

Figure 3. Effect of reactant concentration on the initial liquid-phase esterification rate: (a) $C_{MeOH,0}$ = 14.6 M and (b) $C_{HAc,0}$ = 2.5 M (r_0 in units of mol L^{-1} min^{-1}).

Acetic acid (99.7 wt %), anhydrous methanol (99.9 wt %), and methyl acetate (99 wt %) were obtained from Sigma-Aldrich and used without further purification. Tetrahydrofuran (THF, 99.9 wt %) was utilized as an inert solvent and obtained from the same vendor. In order to determine the effect of water on WZ700, high-performance liquid chromatography (HPLC)-grade water (Acros Organics) was employed.

Gas-phase esterification reactions were carried out in the temperature range of 100−140 °C using a stainless steel differential reactor (i.d. = 0.7 cm). Two layers of quartz wool were used to hold the solid catalyst bed in place. In order to obtain a differential conversion and to minimize heat transfer

Table 2. Apparent Reaction Orders with Respect to Acetic Acid (α) and Methanol (β) for WZ700 at Different Reaction Temperatures

		α[a]		β[a]		concentration range	
reaction temperature (°C)	phase	initially	SS[b]	initially	SS[b]	HAc	MeOH
40	liquid	0.61	NA	0.95	NA	1.6−6.3 M	6.6−17.3 M
60	liquid	0.70	NA	0.98	NA	1.6−3.1 M	6.9−17.3 M
110	gas	0.86	0.86	0.28	0.31	0.4−0.6 mM	0.4−0.9 mM
120	gas	0.74	0.72	−0.25	−0.20	0.2−0.8 mM	0.2−0.8 mM
130	gas	0.69	1.20	−0.58	−0.38	0.4−0.6 mM	0.4−0.8 mM

[a] Error of measurements ± 0.09. [b] SS = steady state (reaction order calculated from SS activity).

effects and nonuniform flow, WZ700 was mixed with an inert solid having negligible activity toward esterification (0.02 (g of WZ700)/0.28 (g of α-Al_2O_3)). Then the solid mixture was pretreated in situ at 315 °C under air flow for 2 h in order to desorb/burn out any impurities. Subsequently, the reaction system was cooled and then reheated to the desired reaction temperature (100−140 °C) under flowing helium. A mixed-gas stream of acetic acid and methanol vapor in helium (120 mL/min) coming from gas saturators was then introduced into the differential reactor. The concentration of the input materials (reactor bypass) and methyl acetate was analyzed using a Varian CP-3380 GC equipped with a CPWAX 52CB Varian fused silica capillary column (60 m × 0.53 mm × 1 μm) and a flame-ionization detector (FID) using a temperature program previously described.[28]

Liquid-phase esterification was carried out using an isothermal, well-mixed (1790 rpm) Parr batch reactor (model 4590). The temperature range studied was 21−60 °C. Acetic acid and catalyst were mixed and heated to the reaction temperature, followed by the addition of methanol to start the reaction. In order to find the apparent reaction orders, THF was utilized as an inert diluent so that the concentration of one reactant could be modified while keeping the total reaction volume constant. Reaction samples (∼0.1 mL) were periodically taken during reaction, and their chemical compositions were determined as previously described using an HP 6890 GC.[39]

3. Results

3.1. Catalyst Characterization. The tungsten content of WZ700 was found to be 13.4 wt %, in good agreement with the tungsten content reported by the manufacturer (15 wt %). WZ700 exhibited a Brunauer−Emmett−Teller (BET) surface area, BJH pore volume, and average pore size of 95 m^2/g, 0.14 cm^3/g, and 53 Å, respectively. The BET surface areas of the pellet and powder forms of SGN_WZ600 (as received) were essentially the same within experimental error, 126.5 ± 2.5 m^2/g, consistent with the value provided by the pellet manufacturer (128 m^2/g). The estimated BJH pore volumes and average pore sizes were also essentially equivalent, 0.13 cm^3/g and 42 Å, respectively. In a parallel study to the present one regarding the effect of calcination temperature on WZ activity, we found that the formation of polymeric tungsten species enhances the esterification rate. Therefore, the SGN_WZ600 sample was recalcined at 700 °C (SGN_WZ700) to obtain an active material more comparable to WZ700. After recalcination, SGN_WZ700 exhibited equivalent structural properties to WZ700. The BET surface area, BJH pore volume, and average pore size for SGN_WZ700 were found to be 97 m^2/g, 0.14 cm^3/g, and 56 Å, respectively.

For both WZ700 and SGN_WZ700, powder X-ray diffraction (XRD) results indicated diffraction peaks only for the tetragonal phase of ZrO_2.[28] Also, the characteristic peaks for crystalline WO_3 were not observed, as is typical for this W loading and calcination temperature.[28] For WZ700, the ion-exchange/titration method gave a total acid site concentration of 0.137 meq H^+/g. We have shown that acid site concentrations determined by this method better correlate to the catalytic activity.[28]

3.2. Exclusion of Mass Transport Effects. For gas-phase esterification, we have previously shown that heat and mass diffusional limitations are negligible under the reaction conditions used here.[31] For liquid-phase esterification, the observed reaction rate was shown to be independent of external diffusion limitations for stirrer speeds > 850 rpm.[26] An agitation rate of 1790 rpm was utilized for this study to rule out the presence of heat and mass transport limitations. The effect of pore diffusion was examined by carrying out the reaction using various particle sizes (see Experimental Section). Figure 1 shows the results of the pore diffusion experiments including the reaction rate for the pelleted catalyst. Within experimental error, pore diffusion effects appeared to be negligible for particle sizes ≤ 0.3 mm. Therefore, only particle sizes ≤ 0.11 mm were used for further kinetic studies to ensure that the reaction rate observed would not be limited by internal diffusion of the reactants in the catalyst pores.

3.3. Power Law Expressions and Activation Energies. 3.3.1. Liquid-Phase Reaction. 3.3.1.1. Autocatalysis. Prior to the liquid-phase kinetic studies using solid catalysts, control experiments (solid catalyst-free) were carried out so as to quantify the catalytic role of the weak carboxylic acid (CH_3-COOH) in the reaction. The contribution from the stainless steel walls of the reactor to catalysis was determined to be negligible by performing a control experiment using a glass liner. Esterification reaction rates were determined from initial reaction rate data (acetic acid conversion < 3%), where the slope of the methyl acetate concentration vs time plot was essentially linear in the 21−60 °C temperature range. Initially, since the concentration of products is low, any change in the reaction rate results primarily from the forward reaction (i.e., esterification). Pöpken et al.[8] provided evidence for autocatalysis occurring via molecular acetic acid as opposed to via a fully solvated proton. Since acetic acid esterification with methanol at low temperatures has been found to be approximately first order in each of the two reactants and first order in the catalyst (acetic acid),[8] an overall third-order power law expression can be used to accurately describe the autocatalyzed initial esterification rate as follows,

$$-\left(\frac{dC_{HAc}}{dt}\right)_0 = r_0 = k_{auto} C_{HAc,0}{}^2 C_{MeOH,0} \qquad (1)$$

where k_{auto} denotes the esterification rate constant for autocatalysis and $C_{HAc,0}$ and $C_{MeOH,0}$ represent the initial molar concentrations of acetic acid and methanol, respectively. The reaction rates and values of the autocatalyzed esterification rate constants are provided in Table 1. At 60 °C, k_{auto} was determined to be 13.7 × 10^{-6} ± 1.2 × 10^{-6} mol^{-2} L^2 min^{-1}, in excellent agreement with the literature.[9] The Arrhenius plot of the reaction

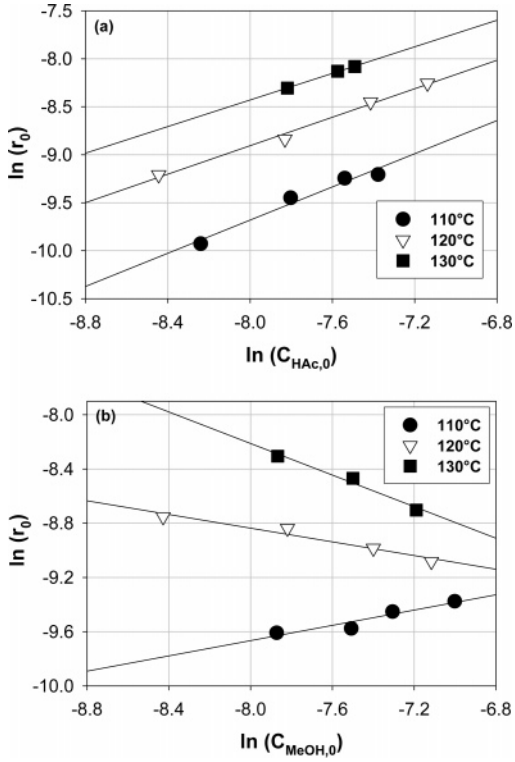

Figure 4. Effect of reactant concentration on the initial gas-phase esterification rate: (a) $C_{MeOH,0} = 0.4$ mmol/L and (b) $C_{HAc,0} = 0.4$ mmol/L.

results (Figure 2) was used to obtain the apparent activation energy of the autocatalyzed reaction. E_a was found to be 53.1 ± 2.4 kJ/mol, lower than a previously reported theoretical value ($E_a = 73.6$ kJ/mol in the 40−60 °C temperature range[8]).

3.3.1.2. Solid-Catalyzed Esterification. In order to obtain accurate activation energies and reaction orders for the solid-catalyzed liquid-phase esterification reaction

$$CH_3COOH + CH_3OH \overset{H^+}{\longleftrightarrow} CH_3COOCH_3 + H_2O \quad (2)$$

the contribution of autocatalysis was subtracted from the observed initial reaction rate as follows,

$$\left\{-\left(\frac{dC_{HAc}}{dt}\right)_0 - k_{auto}C_{HAc,0}{}^2C_{MeOH,0}\right\} = r_0 = k_hC_{cat}C^{\alpha}_{HAc,0}\,C^{\beta}_{MeOH,0} \quad (3)$$

where k_h denotes the apparent reaction rate constant for the heterogeneous-catalyzed esterification, C_{cat} is the concentration of the solid catalyst ($C_{cat} = 18.5$ g/L), and α and β designate the apparent reaction orders with respect to acetic acid and methanol, respectively. In order to prevent autocatalysis in the liquid phase during ramping to the desired reaction temperature, acetic acid, THF, and WZ700 were first heated to the desired reaction temperature and then methanol was added to the mixture. In the temperature range studied for liquid-phase esterification (21−60 °C), the contribution of autocatalysis was typically <10% of the total conversion in the presence of WZ700 (unless the concentration of acetic acid was very high). Figure 3 provides the initial liquid-phase esterification rate data obtained at different reactant concentrations. For both reaction temperatures studied (40 and 60 °C), the reaction order with respect to methanol (β) was found to be close to 1 (0.95 and 0.98, respectively) (see Table 2). The values of α were also found to be positive, 0.61 ± 0.09 and 0.70 ± 0.09 at reaction

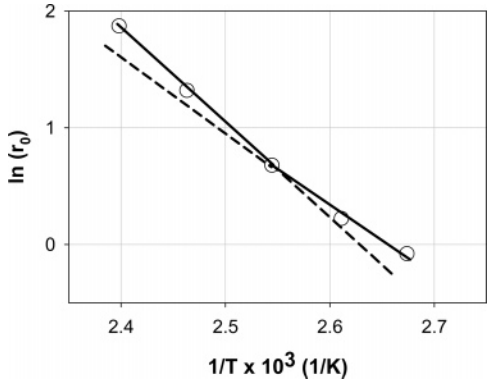

Figure 5. Arrhenius plot for the gas-phase esterification of acetic acid with methanol in the 100−140 °C temperature range using WZ700 (reaction rate in μmol g_{cat}^{-1} s^{-1}). Average error in the measurement: ln r_0 ± 0.16.

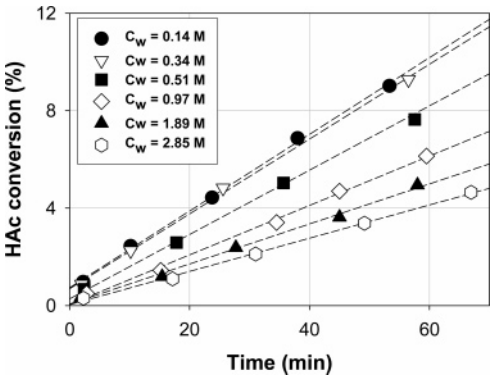

Figure 6. Effect of water on the catalytic activity of WZ700 for the esterification of acetic acid with methanol at 60 °C ($C_{cat} = 1.09$ g/54 mL, $C_{HAc,0} = 3$ M, and $C_{MeOH,0} = 6$ M).

temperatures of 40 and 60 °C, respectively. The activation energy for WZ700-catalyzed liquid-phase esterification was determined from an Arrhenius plot for the 21−60 °C temperature range to be 41.0 ± 2.4 kJ/mol (Figure 2). This value is somewhat lower than those previously reported for other solid acid catalysts, such as NafionSAC-13 (51.8 kJ/mol[26]) and Amberlyst15 (61.5 kJ/mol[8]). However, none of these studies took into account autocatalysis.

3.3.2. Gas-Phase Reaction. For gas-phase esterification, the autocatalysis contribution was found to be negligible, as expected from the low concentrations of acetic acid employed (C_{HAc} typically equal to 0.40 mmol/L). Thus, the second term on the left-hand side of eq 3 can be neglected,

$$-\left(\frac{dC_{HAc}}{dt}\right)_0 = r_0 = k_hC_{cat}C^{\alpha}_{HAc,0}\,C^{\beta}_{MeOH,0} \quad (4)$$

The reaction rate results shown in Figure 4 were used to determine the orders of reaction using eq 4 (see Table 2). Because preliminary results had indicated that, at higher reaction temperatures, the order of reaction for methanol is negative, concentrations around stoichiometric (rather than using a large excess of methanol) were used to determine reaction orders. The gas-phase reaction was positive order in acetic acid (α) (0.86−0.69) for the temperature range of 110−130 °C, similar to the orders of reaction in the liquid phase (0.61−0.70). While the value of α remained fairly constant (0.76 ± 0.09), the reaction order for methanol (β) decreased with increasing temperature, going from ∼0.98 in the liquid phase (at 40−60 °C) to 0.28 (110 °C), −0.25 (120 °C), and −0.58 (130 °C) in the gas phase. The apparent reaction order results for these higher temperatures compare well with recently obtained gas-

Table 3. Possible Esterification Reaction Mechanistic Steps on Tungstated Zirconia[a]

step		k_j	k_{-j}	K_j
(1) carboxylic acid ad/desorption	$HAc + S \leftrightarrow HAc{\cdot}S$	k_{HAc}	k_{-HAc}	K_{HAc}
(2) alcohol ad/desorption	$MeOH + S \leftrightarrow MeOH{\cdot}S$	k_{MeOH}	k_{-MeOH}	K_{MeOH}
(3) surface reaction	*b*	k_R	k_{-R}	K_R
(4) water ad/desorption	$H_2O + S \leftrightarrow H_2O{\cdot}S$	k_w	k_{-w}	K_w
(5) ester ad/desorption	$MeAc + S \leftrightarrow MeAc{\cdot}S$	k_{MeAc}	k_{-MeAc}	K_{MeAc}

[a] S represents the vacant acid sites; MeAc denotes methyl acetate; and HAc·S, MeOH·S, MeAc·S, and $H_2O{\cdot}S$ designate the adsorbed species. K_j, k_j and k_{-j} stand for the reaction or adsorption equilibrium constant, forward reaction or adsorption rate constant, and reverse reaction or desorption rate constant, respectively. [b] (i) = Single site with adsorbed alcohol reacting: $HAc + MeOH{\cdot}S \leftrightarrow MeAc{\cdot}S + H_2O$. (ii) = Single site with adsorbed carboxylic acid reacting: $HAc{\cdot}S + MeOH \leftrightarrow MeAc{\cdot}S + H_2O$. (iii) = Dual-site adsorbed carboxylic acid and alcohol reacting: $HAc{\cdot}S + MeOH{\cdot}S \leftrightarrow MeAc{\cdot}S + H_2O{\cdot}S$.

phase esterification data using silica-supported Nafion (SAC-13) acquired in our laboratory.[40] For that catalyst, the reaction order with respect to methanol evolved from 0.2 to −0.9 as the esterification temperature increased from 90 to 130 °C. Similarly, Nijhuis et al.[25] found that increasing the concentration of 1-octanol in the esterification of hexanoic acid at 150 °C resulted in a decrease in the reaction rate (apparent negative first-order reaction in the alcohol).

Reaction rates determined in the 100−140 °C temperature range were used to obtain an Arrhenius plot for the gas-phase esterification of acetic acid (Figure 5). For this set of experiments, an equimolar reactant ratio was employed ($C_{HAc,0} = C_{MeOH,0} = 0.40$ mmol/L). It was observed that two distinctive slopes could be calculated from the Arrhenius correlation, corresponding to apparent activation energies of $E_{a,\,100-120°C} = 48.4 \pm 12.2$ kJ/mol (comparable to that for liquid-phase reaction in the range 21−60 °C) and $E_{a,\,120-140°C} = 67.8 \pm 3.6$ kJ/mol. Given the lack of heat or mass transfer effects[31] (reaction is slightly exothermic and acetic acid conversion was typically <11%), the apparent change in activation energy together with the significant changes in reaction order (as temperature increased) suggests either a change in the reaction mechanism or, as it turns out more likely, a change in the rate-limiting step (discussed more in detail later).

3.4. Effect of Water on Tungstated Zirconia Catalytic Activity. In order to investigate the effect of water on WZ700 catalytic activity, initial liquid-phase esterification rates (60 °C, acetic acid conversion < 10%) were collected using different initial water concentrations. Since water is produced by the esterification reaction, the concentration of water (C_w) was estimated by taking the sum of the added water concentration ($C_{w,a}$) and the average concentration of water produced by reaction,

$$C_w = C_{w,a} + C_{HAc}\bar{x} \tag{5}$$

where $\bar{x}$ is the average acetic acid conversion. Figure 6 shows that the conversion of acetic acid after 1 h of reaction decreased from ∼10% conversion (for $C_w = 0.14$ M) to 4% (for $C_w = 2.85$ M) with increasing water concentration. For this set of experiments, C_{cat} was 24.2 g/L, THF was used to keep the reaction volume constant to 30 mL, and acetic acid and methanol initial concentrations were 3 and 6 M, respectively. It has previously been shown that there is a negligible influence of the reverse hydrolysis reaction on the initial esterification rate under the experimental conditions utilized.[9] Therefore, the observed variations on the initial esterification rate can be exclusively attributed to the impact of water on the solid catalyst.[26]

4. Discussion

It is well-known that WZ may exhibit a complex surface consisting of polymeric tungsten oxide species, crystalline WO_3, and compounds formed by the interaction of tungsten species with the zirconia support ($Zr(WO_4)_2$) depending on the preparation and activation conditions.[41] In a parallel study to the present one regarding the effect of calcination temperature on WZ activity, we concluded that esterification reactions are primarily carried out by Brønsted acid sites on WZ (calcined at 800 °C).[28] Similar results were obtained for the catalyst calcined at 700 °C (WZ700).[31] Therefore, the fact that a single type of site dominates the macroscopic behavior enables us to model these reactions as if they occur on an ideal surface consisting of only one type of active site. Bearing this consideration in mind, simple mechanistic expressions for esterification can be derived.

4.1. Esterification Mechanism on Tungstated Zirconia. In this study, for completeness, all three possible esterification reaction mechanisms were examined: (i) a single-site mechanism with adsorbed alcohol reacting, (ii) a single-site mechanism with adsorbed carboxylic acid reacting, and (iii) a dual-site mechanism. The elementary reaction steps for these mechanisms are shown in Table 3. Since the orders of reaction for both acetic acid and methanol were determined to be <1, the competitive adsorption of all species but THF (slightly polar solvent) was considered in the analysis. The reaction rate expressions were derived using the Langmuir−Hinshelwood (LH) approach and are provided in Table 4.

To evaluate which is the most likely mechanism, a methodical comparison of predicted reaction orders versus observed kinetics behavior was undertaken. Because the observed methanol reaction order (β) was found to evolve from positive to negative (Table 2) and mechanism (i) (single-site methanol adsorbed) cannot describe a negative reaction order in methanol, this possibility was ruled out. On the other hand, mechanism (ii) (single-site acetic acid adsorbed) is able to explain not only a negative reaction order in methanol but also the observed positive reaction order in acetic acid (see (ii-a) and (ii-b)), and likewise for mechanism (iii) (dual site, see (iii-a) and (iii-c)). However, the plot of rate vs methanol concentration was linear and did not exhibit a maximum in rate[12] for the reactant concentrations studied (Table 2). In addition, previous poisoning experiments for acetic acid esterification on silica supported Nafion (SAC-13), a catalyst also with Brønsted acidity, have not supported the existence of a dual-site mechanism.[26] Therefore, we are led to conclude that mechanism (iii) does not accurately describe the observed kinetics for esterification on solid acids or on WZ in particular.

The esterification reaction catalyzed by homogeneous acids is known to proceed via the protonation of the carboxylic acid species. Prior studies have also suggested that solid-acid-catalyzed esterification[12,13,20,25,26] proceeds via a single-site mechanism, where the acid is adsorbed on the solid acid surface.

To further check the suitability of mechanism (ii) (single site with adsorbed acetic acid reacting), a more general expression for any extent of the reaction was derived (similarly to

Table 4. Reaction Rate Expressions for the Potential Esterification Reaction Mechanisms Derived Using the Langmuir−Hinshelwood Approach

mech.	RDS	reaction rate expression	initial rate expression[a]
(i)	(a) adsorption of MeOH	rate = $\{k_{MeOH}C_{cat}[C_{MeOH} - (K_{MeAc}C_{MeAc}C_w)/(K_RK_{MeOH}C_{HAc})]/\{1 + K_{HAc}C_{HAc} + K_{MeAc}C_{MeAc} + K_wC_w + (K_{MeAc}C_{MeAc}C_w)/(K_RK_{MeOH}C_{HAc})\}$	rate = $\{k_{MeOH}C_{cat}C_{MeOH}\}/\{1 + K_{HAc}C_{HAc}\}$
	(b) surface reaction	rate = $\{k_RC_{cat}[K_{MeOH}C_{MeOH}C_{HAc} - (K_{MeAc}C_{MeAc}C_w)/(K_R)]\}/\{1 + K_{HAc}C_{HAc} + K_{MeOH}C_{MeOH} + K_{MeAc}C_{MeAc} + K_wC_w\}$	rate = $\{k_RC_{cat}K_{MeOH}C_{MeOH}C_{HAc}\}/\{1 + K_{HAc}C_{HAc} + K_{MeOH}C_{MeOH}\}$
	(c) desorption of MeAc	rate = $\{k_{MeAc}C_{cat}[(C_{MeAc})/(K_RK_{MeOH}C_{HAc}C_{MeOH})/(K_{MeAc})(C_w)]\}/\{1 + K_{HAc}C_{HAc} + K_{MeOH}C_{MeOH} + K_wC_w + (K_RK_{MeOH}C_{HAc}C_{MeOH})/(C_w)\}$	rate = $k_{-MeAc}C_{cat}$
(ii)	(a) adsorption of HAc	rate = $\{k_{HAc}C_{cat}[C_{HAc} - (K_{MeAc}C_{MeAc}C_w)/(K_RK_{HAc}C_{MeOH})]\}/\{1 + K_{MeOH}C_{MeOH} + K_{MeAc}C_{MeAc} + K_wC_w + (K_{MeAc}C_{MeAc}C_w)/(K_RC_{MeOH})\}$	rate = $\{k_{HAc}C_{cat}C_{HAc}\}/\{1 + K_{MeOH}C_{MeOH}\}$
	(b) surface reaction	rate = $\{k_RC_{cat}[K_{HAc}C_{HAc}C_{MeOH} - (K_{MeAc}C_{MeAc}C_w)/(K_R)]\}/\{1 + K_{HAc}C_{HAc} + K_{MeOH}C_{MeOH} + K_{MeAc}C_{MeAc} + K_wC_w\}$	rate = $\{k_RC_{cat}K_{HAc}C_{HAc}C_{MeOH}\}/\{1 + K_{HAc}C_{HAc} + K_{MeOH}C_{MeOH}\}$
	(c) desorption of MeAc	rate = $\{k_{MeAc}C_{cat}[(C_{MeAc})/(K_RK_{HAc}C_{HAc}C_{MeOH})/(K_{MeAc})(C_w)]\}/\{1 + K_{HAc}C_{HAc} + K_{MeOH}C_{MeOH} + K_wC_w + (K_RK_{HAc}C_{HAc}C_{MeOH})/(C_w)\}$	rate = $k_{-MeAc}C_{cat}$
(iii)	(a) adsorption of HAc	rate = $\{k_{HAc}C_{cat}[C_{HAc} - (K_{MeAc}C_{MeAc}K_wC_w)/(K_RK_{HAc}K_{MeOH}C_{MeOH})]\}/\{1 + K_{MeOH}C_{MeOH} + K_{MeAc}C_{MeAc} + K_wC_w + (K_{MeAc}C_{MeAc}K_wC_w)/(K_RK_{MeOH}C_{MeOH})\}$	rate = $\{k_{HAc}C_{cat}C_{HAc}\}/\{1 + K_{MeOH}C_{MeOH}\}$
	(b) adsorption of MeOH	rate = $\{k_{MeOH}C_{cat}[C_{MeOH} - (K_{MeAc}C_{MeAc}K_wC_w)/(K_RK_{MeOH}K_{HAc}C_{HAc})]\}/\{1 + K_{HAc}C_{HAc} + K_{MeAc}C_{MeAc} + K_wC_w + (K_{MeAc}C_{MeAc}K_wC_w)/(K_RK_{HAc}C_{HAc})\}$	rate = $\{k_{MeOH}C_{cat}C_{MeOH}\}/\{1 + K_{HAc}C_{HAc}\}$
	(c) surface reaction	rate = $\{k_RC_{cat}^2[K_{HAc}K_{MeOH}C_{HAc}C_{MeOH} - (K_wC_wK_{MeAc}C_{MeAc})/(K_R)]\}/\{(1 + K_{HAc}C_{HAc} + K_{MeOH}C_{MeOH} + K_wC_w + K_{MeAc}C_{MeAc})^2\}$	rate = $\{k_RC_{cat}^2K_{HAc}K_{MeOH}C_{HAc}C_{MeOH}\}/\{(1 + K_{HAc}C_{HAc} + K_{MeOH}C_{MeOH})^2\}$
	(d) desorption of H_2O	rate = $\{k_wC_{cat}[C_w - (K_RK_{HAc}K_{MeOH}C_{HAc}C_{MeOH})/(K_wK_{MeAc}C_{MeAc})]\}/\{1 + K_{HAc}C_{HAc} + K_{MeOH}C_{MeOH} + K_{MeAc}C_{MeAc} + (K_RK_{HAc}K_{MeOH}C_{HAc}C_{MeOH})/(K_{MeAc}C_{MeAc})\}$	rate = $k_{-w}C_{cat}$
	(e) desorption of MeAc	rate = $\{k_{MeAc}C_{cat}[C_{MeAc} - (K_RK_{HAc}K_{MeOH}C_{HAc}C_{MeOH})/(K_{MeAc}K_wC_w)]\}/\{1 + K_{HAc}C_{HAc} + K_{MeOH}C_{MeOH} + K_wC_w + (K_RK_{HAc}K_{MeOH}C_{HAc}C_{MeOH})/(K_wC_w)\}$	rate = $k_{-MeAc}C_{cat}$

[a] Valid only for negligible C_w and C_{MeAc}.

previously proposed[42]) considering reaction steps 1 and 3ii (in Table 3) to be rate-limiting over the temperature range studied (as evidenced in the shift of the power law dependence). Writing

$$\text{rate} = r_1 = k_{HAc}C_{HAc}C_S - k_{-HAc}C_{HAc\cdot S} \tag{6}$$

$$\text{rate} = r_3 = k_RC_{HAc\cdot S}C_{MeOH} - k_{-R}C_{MeAc\cdot S}C_w \tag{7}$$

where r_n denotes the overall reaction rate of the n step (in Table 3). We know that, at steady state, $r_1 = r_3 = \text{rate}$. Considering all other reaction steps to be fast and, therefore, in pseudo-equilibrium, $r_{f2} \approx r_{r2}$, $r_{f4} \approx r_{r4}$, $r_{f5} \approx r_{r5}$ (forward and reverse reactions are approximately equal), then:

$$C_{MeOH\cdot S} = K_{MeOH}C_{MeOH}C_S \tag{8a}$$

$$C_{w\cdot S} = K_wC_wC_S \tag{8b}$$

$$C_{MeAc\cdot S} = K_{MeAc}C_{MeAc}C_S \tag{8c}$$

The concentration of adsorbed acetic acid can be obtained by equating eqs 6 and 7, and introducing eq 8c:

$$C_{HAc\cdot S} = \left(\frac{k_{HAc}C_{HAc} + k_{-R}K_{MeAc}C_{MeAc}C_w}{k_RC_{MeOH} + k_{-HAc}}\right)C_S \tag{9}$$

By further substitution of eq 9 into eq 6 and using the concentration of available sites (C_S) calculated from a site mass balance, we obtain

$$\text{rate} = \frac{k_Rk_{HAc}C_{cat}\left(C_{HAc}C_{MeOH} - \frac{C_{MeAc}C_w}{K_e}\right)}{(k_RC_{MeOH} + k_{-HAc})\left(1 + \frac{k_{HAc}C_{HAc} + k_{-R}K_{MeAc}C_{MeAc}C_w}{k_RC_{MeOH} + k_{-HAc}} + K_{MeOH}C_{MeOH} + K_wC_w + K_{MeAc}C_{MeAc}\right)} \tag{10}$$

where $K_e = K_RK_{HAc}/K_{MeAc}$. Initially, when the concentration of products is negligible, eq 10 reduces to

$$\text{rate} = \frac{k_Rk_{HAc}C_{cat}C_{HAc}C_{MeOH}}{(k_RC_{MeOH} + k_{-HAc})\left(1 + \frac{k_{HAc}C_{HAc}}{k_RC_{MeOH} + k_{-HAc}} + K_{MeOH}C_{MeOH}\right)} \tag{11}$$

identical to the initial rate expression that can be derived using the pseudo-steady-state approximation.[26,31] Now, we extend this analysis to the range of operating conditions examined: low to high temperature.

Table 5. Sum of Square Residuals for the Kinetic Data Plotted According to Linearized Rate Expressions

	R^2			
reaction temperature (°C)	eq 13	eq 15	eq 17	eq 18
40	0.980	0.978	0.978	0.996
60	0.997	0.974	0.995	0.992
110	0.947	0.928[a]	0.982	0.982
120	0.996	0.992	0.982	0.986[a]
130	0.997	0.997	0.999	0.949[a]

[a] The fit of the equation resulted in a negative slope, providing evidence for the unsuitability of the particular equation to describe the kinetics of the reaction.

For high-temperature reaction (gas-phase esterification), it appears, based on the power law exponents, that acetic acid adsorption is controlling the kinetic behavior. Under these conditions, it is reasonable to suggest that $k_{HAc}C_{HAc} \ll (k_R C_{MeOH} + k_{-HAc})$ and eq 11 can be approximated by

$$\text{rate} = \frac{k_{HAc}k_R C_{cat} C_{MeOH} C_{HAc}}{(k_{-HAc} + k_R C_{MeOH})(1 + K_{MeOH} C_{MeOH})} \quad (12)$$

The rate data were fit to linearized forms of eq 12 that required experiments conducted either at a constant methanol concentration ($C_{MeOH} = 0.4$ mmol/L),

$$\text{rate} = \frac{k_{HAc}k_R C_{cat} C_{MeOH}}{(k_{-HAc} + k_R C_{MeOH})(1 + K_{MeOH} C_{MeOH})} \cdot C_{HAc} \quad (13)$$

or constant acetic acid concentration ($C_{HAc} = 0.4$ mmol/L),

$$\frac{1}{\text{rate}} = \frac{k_{-HAc}}{k_R k_{HAc} C_{cat} C_{HAc}} \cdot \frac{1}{C_{MeOH}} + \frac{k_{-HAc}K_{MeOH} + k_R}{k_R k_{HAc} C_{cat} C_{HAc}} + \frac{k_R K_{MeOH}}{k_R k_{HAc} C_{cat} C_{HAc}} \cdot C_{MeOH} \quad (14)$$

Equation 14 can be linearized since acetic acid adsorption is controlling and the reaction terms are large compared to the adsorption/desorption terms; thus, the first term on the right-hand side of eq 14 is small compared to the other two terms and can be neglected. Therefore,

$$\frac{1}{\text{rate}} = \frac{k_{-HAc}K_{MeOH} + k_R}{k_R k_{HAc} C_{cat} C_{HAc}} + \frac{k_R K_{MeOH}}{k_R k_{HAc} C_{cat} C_{HAc}} \cdot C_{MeOH} \quad (15)$$

Table 5 provides the sum of square residuals (R^2 values) for the reaction rate data plotted according to eqs 13 and 15. The goodness of the fit of these equations at high reaction temperatures (120 and 130 °C) suggests that mechanism (ii) is suitable for describing high-temperature esterification kinetics in the gas phase. Under these conditions, methanol may compete more strongly for active sites, making it less likely for acetic acid to adsorb on the solid surface.

The kinetic data obtained at 110 °C did not show a good correlation ($R^2 < 0.95$) using either of the previously derived linearizations, eq 13 or eq 15. Evidently, the importance of the other terms in eq 11 increases as the reaction temperature decreases to the point where proton-donation from Brønsted acid sites (step 1) proceeds more rapidly than nucleophilic substitution (step 3). Under these conditions, both k_{HAc} and k_{-HAc} may be greater than $k_R C_{MeOH}$ and eq 11 reduces to the same expression originally obtained using the LH approach for surface reaction being the rate-determining step (RDS):

$$\text{rate} = \frac{k_R K_{HAc} C_{cat} C_{MeOH} C_{HAc}}{(1 + K_{MeOH} C_{MeOH} + K_{HAc} C_{HAc})} \quad (16)$$

Linearization of eq 16 gives

$$\frac{1}{\text{rate}} = \frac{1 + K_{MeOH} C_{MeOH}}{k_R K_{HAc} C_{cat} C_{MeOH}} \cdot \frac{1}{C_{HAc}} + \frac{K_{HAc}}{k_R K_{HAc} C_{cat} C_{MeOH}} \quad (17)$$

and

$$\frac{1}{\text{rate}} = \frac{1 + K_{HAc} C_{HAc}}{k_R K_{HAc} C_{cat} C_{HAc}} \cdot \frac{1}{C_{MeOH}} + \frac{K_{MeOH}}{k_R K_{HAc} C_{cat} C_{HAc}} \quad (18)$$

Linear fits of 1/rate vs $1/C_x$ (x = MeOH, HAc), where the concentration of the other reactants was held constant and only initial rates were used, provide poor correlations for esterification carried out at 110−130 °C (Table 5). In contrast, for low-temperature esterification (liquid phase, 40 and 60 °C), both eqs 17 and 18 accurately describe the observed rate behavior (Table 5). Therefore, at lower esterification temperatures, it would appear that surface reaction dominates the kinetic behavior.

In summary, the reaction mechanism appears to be the same for both gas and liquid phases. Although MeOH adsorbs, reaction to form the ester on WZ occurs between adsorbed acetic acid and nonadsorbed MeOH, just like for the homogeneously catalyzed reaction. At lower temperatures where this reaction is the RDS, MeOH is part of the driving force of the reaction. Thus, even though the MeOH adsorption term in the denominator reduces the positive order for MeOH, the overall order for MeOH still remains almost 1. However, as the temperature rises above 110 °C, the order of reaction for MeOH became negative because of the RDS becoming the adsorption of acetic acid. Thus, the only contribution of MeOH to the rate of reaction is negative because of its adsorption on sites. The driving force is only the concentration of acetic acid. The adsorption of MeOH acts only to poison the reaction since there is no evidence that reaction ever proceeds via adsorbed MeOH. The order of reaction can change significantly depending on the RDS in a mechanism, as it does in this case and as is shown in Table 4.

4.2. Effect of Water on Tungstated Zirconia. Until this point, we have discussed only the initial esterification rates; however, one important issue with esterification is the formation of water. The presence of water not only hinders the activity of the catalyst (as shown in Figure 6) but also has the potential to lower the yield of the alkyl ester product (e.g., biodiesel) by shifting the chemical equilibrium toward the formation of carboxylic acids.[43]

The effect of water on WZ700 was compared to that effect reported for NafionSAC-13[26] under the same reaction conditions (liquid phase, 60 °C). Both acid catalysts possess comparable acid site densities (137 and 130 μeq/g, respectively). As shown in Figure 7, both solid catalysts exhibited an analogous deactivation within experimental error in the presence of water. The similar decrease in the esterification rate is not surprising as it is known that these catalysts have similar acid strengths. Liu et al.[9] previously suggested that, for homogeneous-catalyzed esterification, the decrease in the esterification rate with increasing water concentration originates from the solvation of the acid catalyst proton ($H_2O{-}H^+HSO_4^-$), which results in a decrease in acid strength.

The value of the equilibrium constant obtained in this study was $K_e = 5.26 \pm 0.99$, comparable to those reported in the literature (e.g., $K_e = 5.20$[44] and $K_e = 5.65$[45]). Hence, the

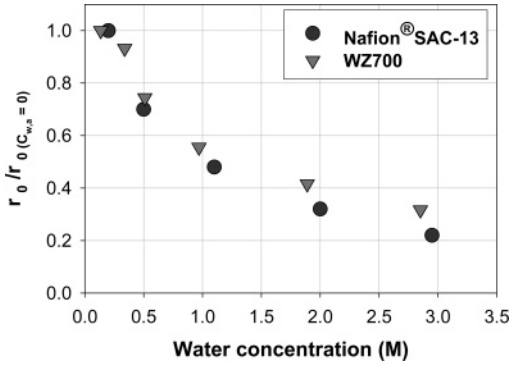

Figure 7. Comparison of the effect of water on the initial esterification rate using different acid catalysts (C_{cat} = 1.09 g/54 mL, $C_{HAc,0}$ = 3 M, and $C_{MeOH,0}$ = 6 M). Experimental error ± 2%. The data for NafionSAC-13 is from ref 26.

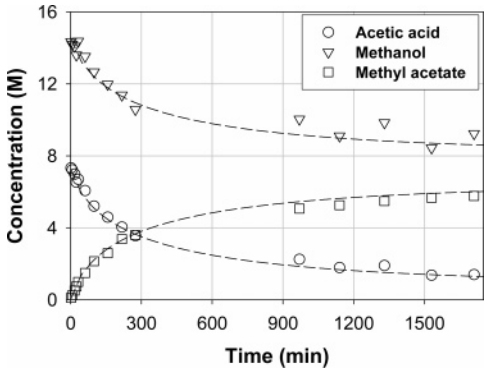

Figure 8. Esterification of acetic acid with methanol at 60 °C with C_{cat} = 60 g/L. Symbols = experimental data, and dashed lines = eq 22 prediction.

Table 6. Kinetic Parameters Estimated for the Esterification of Acetic Acid with Methanol in the Liquid Phase

parameter	40 °C	60 °C	units
k_R	4.2×10^{-5}	10.3×10^{-5}	L g_{cat}^{-1} min^{-1}
k_{HAc}	11.2	20.6	L g_{cat}^{-1} min^{-1}
k_{-HAc}	56.9	103.1	mol g_{cat}^{-1} min^{-1}
K_{MeOH}	0.01	0.08	M^{-1}
$K_{HAc} = k_{HAc}/k_{-HAc}$	0.20	0.20	M^{-1}

maximum concentration of water that could be produced by reaction under the experimental conditions was estimated to be 2.6 M. Thus, it can be concluded that only 35% of the catalyst activity would be available as reaction reaches chemical equilibrium (assuming no other deactivation). Baertsch et al.[46] also found that the presence of the highest amount of water that could possibly be produced by reaction (2-butanol dehydration carried out at 100 °C on WZ calcined at 700 °C) significantly reduced the initial alcohol dehydration rate (by 90%).

In this work, the reaction configuration that allowed studying the effect of the accumulation of water was the batch system. Also, at 60 °C and below, we found that the reaction was strictly controlled by a single reaction step (surface reaction) as opposed to the RDS transition found at higher reaction temperatures. Therefore, because of the simpler rate expression at the lower temperatures, we can conveniently calculate relevant kinetic parameters in the liquid phase. A linear least-squares fit of the initial kinetic data (eqs 17 and 18) was used for the first estimation. For a reaction temperature of 40 °C, the first estimates of kinetic parameters k_R, K_{MeOH}, and K_{HAc} were determined to be $6 \pm 3 \times 10^{-6}$ L g_{cat}^{-1} min^{-1}, 0.023 M^{-1}, and 0.286 M^{-1}, respectively. For a reaction temperature of 60 °C, the first estimates of kinetic parameters k_R, K_{MeOH}, and K_{HAc} were determined to be $10 \pm 5 \times 10^{-6}$ L g_{cat}^{-1} min^{-1}, 0.015 M^{-1}, and 0.250 M^{-1}, respectively. This information was then used as the initial guess for obtaining the kinetic parameters for eq 11 using a nonlinear regression procedure (L-M, Polymath 5.1). The results are summarized in Table 6.

The catalytic activity inhibition by water can be expressed mathematically by considering the competitive adsorption of water molecules on the active sites. Under these reaction conditions (initial reaction with water added), eq 10 can be approximated by

$$\text{rate} = \frac{k_R K_{HAc} C_{cat} C_{MeOH} C_{HAc}}{(1 + K_{HAc} C_{HAc} + K_{MeOH} C_{MeOH} + K_w C_w)} \quad (19)$$

The set of experiments with variable C_w and constant initial concentrations of acetic acid (3 M) and methanol (6 M) can now be fitted to a linearized form of eq 19 to obtain the water adsorption equilibrium constant (K_w) as follows:

$$\frac{1}{\text{rate}} = \frac{1 + K_{MeOH} C_{MeOH} + K_{HAc} C_{HAc}}{k_R K_{HAc} C_{cat} C_{MeOH} C_{HAc}} + \frac{K_w}{k_R K_{HAc} C_{cat} C_{MeOH} C_{HAc}} C_w \quad (20)$$

Using the slope/intercept ratio of eq 20 and the estimated values of the reactant adsorption equilibrium constants based on the initial rate measurements in the absence of added water (Table 6), K_w was found to be 1.87 M^{-1}, which indicates that even low concentrations of water may appreciably impact the observed esterification rate. However, WZ700 may be more resistant to water deactivation than other solid acids because the value of K_w is lower than those reported for other acid catalysts, such as NafionSAC-13 (K_w = 3.11 M^{-1} [26]) and Amberlite IR-120 (K_w = 3.20 M^{-1} [24]) at the same reaction temperature (60 °C).

Equation 21 provides a general expression over a wide range of conversions for the esterification rate considering the effect of the reverse reaction under these conditions (from eq 10):

$$\text{rate} = \frac{k_R K_{HAc} C_{cat} \left(C_{MeOH} C_{HAc} - \frac{C_{MeAc} C_w}{K_e} \right)}{(1 + K_{MeOH} C_{MeOH} + K_{HAc} C_{HAc} + K_{MeAc} C_{MeAc} + K_w C_w)} \quad (21)$$

The contribution of the adsorption of the ester product has been previously shown to be negligible (small K_{MeAc}).[24,26] Thus, normally the term $K_{MeAc} C_{MeAc} \rightarrow 0$. With this simplification, eq 21 reduces to

$$\text{rate} = \frac{k_R K_{HAc} C_{cat} \left(C_{MeOH} C_{HAc} - \frac{C_{MeAc} C_w}{K_e} \right)}{(1 + K_{MeOH} C_{MeOH} + K_{HAc} C_{HAc} + K_w C_w)} \quad (22)$$

In order to corroborate the suitability of the estimated kinetic parameters for predicting liquid-phase esterification, eq 22 was solved using the values provided in Table 6, C_{cat} = 60 g/L, K_e = 5.26, $C_{HAc,0}$ = 7.3 M, $C_{MeOH,0}$ = 14.6 M, and $C_{w,0} = C_{MeAc,0}$ = 0 in Polymath 5.1 (RFK45 method). As shown in Figure 8, eq 22 (dashed lines) successfully predicts the results (open symbols) during the entire course of an independent reaction experiment from 0 to 89% acetic acid conversion. This result confirms our previous suggestion about the importance of the

competitive adsorption of water molecules ($K_w/K_{HAc} \approx 10$) on the active sites.

5. Conclusions

The kinetics of high (gas-phase) and low (liquid-phase) temperature esterification of acetic acid with methanol catalyzed by tungstated zirconia were investigated. The kinetic measurements were obtained under conditions where external and internal mass limitations were able to be ruled out. In order to estimate accurate kinetic parameters, the contribution of the weak carboxylic acid for catalyzing the esterification reaction in the liquid phase was also examined. For liquid-phase esterification, the activation energy for the autocatalyzed reaction was found to be 12 kJ/mol higher than the solid-catalyzed one. For reaction temperatures ≤ 110 °C, an increase in either the concentration of methanol or acetic acid was found to have a positive impact on the reaction rate, suggesting that surface reaction was the rate-determining step. However, at temperatures ≥ 120 °C, a negative reaction order with respect to methanol indicated that the adsorption of acetic acid became the rate-limiting step in the reaction, perhaps because of increased competitive adsorption by the alcohol. For all reaction temperatures, a single-site mechanism, where the carboxylic acid is first protonated and then reacts with the alcohol (from the fluid phase) was found to be suitable for describing the experimental results. This indicates that there is essentially no difference between gas-phase (higher temperature) and liquid-phase (lower temperature) esterification mechanisms. As the esterification temperature increases, a shift in the rate-determining step from nucleophilic attack (by the alcohol on the adsorbed carboxylic acid) to carboxylic acid adsorption on the catalyst surface would appear to occur. The effect of water on the esterification of acetic acid with methanol was also addressed. As expected, the presence of water decreased the esterification rate as a result of the competitive adsorption of water molecules on the active sites.

Acknowledgment

We gratefully acknowledge the U.S. Department of Agriculture (Award No. 68-3A75-3-147) for financial support. The authors thank Magnesium Electron, Inc. (MEI, Manchester, U.K.) and Saint Gobain NorPro (Stow, OH) for providing the WZ precursor and activated WZ pellets, respectively. The authors are grateful to Prof. Mª Dolores Rovira of the University of Central America (UCA) for her valuable comments on the manuscript.

Literature Cited

(1) Goff, M. J.; Bauer, N. S.; Lopes, S.; Sutterlin, W. R.; Suppes, G. J. Acid-Catalyzed Alcoholysis of Soybean Oil. *J. Am. Oil Chem. Soc.* **2004**, *81*, 415.

(2) Lotero, E.; Liu, Y.; Lopez, D. E.; Suwannakarn, K.; Bruce, D. A.; Goodwin, J. G., Jr. Synthesis of Biodiesel via Acid Catalysis. *Ind. Eng. Chem. Res.* **2005**, *44*, 5353.

(3) Lotero, E.; Goodwin, J. G., Jr.; Bruce, D. A.; Suwannakarn, K.; Liu, Y.; López, D. E. The Catalysis of Biodiesel Synthesis. In *Catalysis*, Vol. 19; Royal Chemistry Society Publishing: Cambridge, U.K., 2006.

(4) Kulkarni, M. G.; Dalai, A. K. Waste Cooking Oil—An Economical Source for Biodiesel: A Review. *Ind. Eng. Chem. Res.* **2006**, *45*, 2901.

(5) Omota, F.; Dimian, A. C.; Bliek, A. Fatty Acid Esterification by Reactive Distillation. Part 2. Kinetics-Based Design for Sulphated Zirconia Catalysts. *Chem. Eng. Sci.* **2003**, *58*, 3175.

(6) Chu, W.; Hu, J.; Xie, Z.; Chen, Q. Design and Elaboration of New Solid Acids for the Synthesis of Butylacetate. *Catal. Today* **2004**, *90*, 349.

(7) Peters, T. A.; Benes, N. E.; Holmen, A.; Keurentjes, J. T. F. Comparison of Commercial Solid Acid Catalysts for the Esterification of Acetic Acid with Butanol. *Appl. Catal., A* **2006**, *297*, 182.

(8) Pöpken, T.; Götze, L.; Gmehling, J. Reaction Kinetics and Chemical Equilibrium of Homogeneously and Heterogeneously Catalyzed Acetic Acid Esterification with Methanol and Methyl Acetate Hydrolysis. *Ind. Eng. Chem. Res.* **2000**, *39*, 2601.

(9) Liu, Y.; Lotero, E.; Goodwin, J. G., Jr. Effect of Water on Sulfuric Acid Catalyzed Esterification. *J. Mol. Catal., A* **2006**, *245*, 132.

(10) Chen, X.; Xu, Z. P.; Okuhara, T. Liquid Phase Esterification of Acrylic Acid with 1-Butanol Catalyzed by Solid Acid Catalysts. *Appl. Catal., A* **1999**, *180*, 261.

(11) Xu, Z. P.; Chuang, K. T. Kinetics of Acetic Acid Esterification over Ion Exchange Catalysts. *Can. J. Chem. Eng.* **1996**, *74*, 493.

(12) Kirumakki, S. R.; Nagaraju, N.; Chary, K. V. R. Esterification of Alcohols with Acetic Acid over Zeolites Hβ, HY and HZSM5. *Appl. Catal., A* **2006**, *299*, 185.

(13) Koster, R.; van der Linden, B.; Poels, E.; Bliek, A. The Mechanism of the Gas-Phase Esterification of Acetic Acid and Ethanol over MCM-41. *J. Catal.* **2001**, *204*, 333.

(14) Roberts, I.; Urey, H. C. Esterification of Benzoic Acid with Methyl Alcohol by Use of Isotopic Oxygen. *J. Am. Chem. Soc.* **1938**, *60*, 2391.

(15) Teo, H. T. R.; Saha, B. Heterogeneous Catalyzed Esterification of Acetic Acid with Isoamyl Alcohol: Kinetic Studies. *J. Catal.* **2004**, *228*, 174.

(16) Palani, A.; Pandurangan, A. Esterification of Acetic Acid over Mesoporous Al-MCM-41 Molecular Sieves. *J. Mol. Catal., A* **2005**, *226*, 129.

(17) Lee, M.-J.; Wu, H.-T.; Kang, C.-H.; Lin, H.-M. Kinetics of Catalytic Esterification of Acetic Acid with Amyl Alcohol over Amberlyst 15. *J. Chem. Eng. Jpn.* **2001**, *34*, 960.

(18) Yu, W.; Hidajat, K.; Ray, A. K. Determination of Adsorption and Kinetic Parameters for Methyl Acetate Esterification and Hydrolysis Reaction Catalyzed by Amberlyst 15. *Appl. Catal., A* **2004**, *260*, 191.

(19) Wu, K.; Chen, Y. An Efficient Two-Phase Reaction of Ethyl Acetate Production in Modified ZSM-5 zeolites. *Appl. Catal., A* **2004**, *257*, 33.

(20) Lilja, J.; Murzin, D. Y.; Salmi, T.; Aumo, J.; Mäki-Arvela, P.; Sundell, M. Esterification of Different Acids over Heterogeneous and Homogeneous Catalysts and Correlation with the Taft Equation. *J. Mol. Catal., A* **2002**, *182*−*183*, 555.

(21) Furuta, S.; Matsuhashi, H.; Arata, K. Biodiesel Fuel Production with Solid Superacids Catalysis in Fixed Bed Reactor under Atmospheric Pressure. *Catal. Commun.* **2004**, *5*, 721.

(22) Furuta, S.; Matsuhashi, H.; Arata, K. Catalytic Action of Sulfated Tin Oxide for Etherification and Esterification in Comparison with Sulfated Zirconia. *Appl. Catal., A* **2004**, *269*, 187.

(23) Ramu, S.; Lingaiah, N.; Prabhavathi Devi, B. L. A.; Prasad, R. V. N.; Suryanarayana, I.; Sai Prasad, P. S. Esterification of Palmitic Acid over Tungsten Oxide Supported on Zirconia Solid Acid Catalyst: Effect of Method of Preparation of the Catalyst on its Structural Stability and Reactivity. *Appl. Catal., A* **2004**, *276*, 163.

(24) Altiokka, M. R.; Çitak, A. Kinetics Study of Esterification of Acetic Acid with Isobutanol in the Presence of Amberlite Catalyst. *Appl. Catal., A* **2003**, *239*, 141.

(25) Nijhuis, T. A.; Beers, A. E. W.; Kapteijn, F.; Moulijn, J. A. Water Removal by Reactive Stripping for a Solid-Acid Catalyzed Esterification in a Monolithic Reactor. *Chem. Eng. Sci.* **2002**, *57*, 1627.

(26) Liu, Y.; Lotero, E.; Goodwin, J. G., Jr. A Comparison of the Esterification of Acetic Acid with Methanol using Heterogeneous vs. Homogeneous Acid Catalysis. *J. Catal.* **2006**, *242*, 278.

(27) Furuta, S.; Matsuhashi, H.; Arata, K. Biodiesel Fuel Production with Solid Amorphous-Zirconia Catalysis in Fixed Bed Reactor. *Biomass Bioenergy* **2006**, *30*, 870.

(28) López, D. E.; Suwannakarn, K.; Goodwin, J. G., Jr.; Bruce, D. A. Esterification and Transesterification on Tungstated Zirconia: Effect of Calcination Temperature. *J. Catal.* **2007**, *247*, 43.

(29) Kulkarni, M. G.; Gopinaht, R.; Meher, L. C.; Dalai, A. K. Solid Acid Catalyzed Biodiesel Production by Simultaneous Esterification and Transesterification. *Green Chem.* **2006**, *8*, 1056.

(30) Rao, K. N.; Sridhar, A.; Lee, A. F.; Tavener, S. J.; Young, N. A.; Wilson, K. Zirconium Phosphate Supported Tungsten Oxide Solid Acid Catalyst for the Esterification of Palmitic Acid. *Green Chem.* **2006**, *8*, 790.

(31) Suwannakarn, K.; Lotero, E.; Goodwin, J. G., Jr. A comparative study of gas phase esterification on solid acid catalysts. *Catal. Lett.* **2007**, *114*, 122.

(32) Thomas, E. R.; Sudborough, J. J. The Direct Esterification of Saturated and Unsaturated Acids. *J. Chem. Soc.* **1912**, *101*, 317.

(33) Taft, R. W. *Steric Effects in Organic Chemistry*; John Wiley & Sons, Inc.: New York, 1956.

(34) Mochida, I.; Anju, Y.; Kato, A.; Seiyama, T. Elimination Reactions on Solid Acid Catalysts. A δ_R LFER Study of the Esterification of Alcohols with Carboxylic Acids over Solid Acid Catalysts. *Bull. Chem. Soc. Jpn.* **1971**, *44*, 2326.

(35) Charton, M. Steric Effects. I. Esterification and Acid Catalyzed Hydrolysis of Esters. *J. Am Oil Chem. Soc.* **1974**, *97*, 1552.

(36) Charton, M. Steric Effects. 7. Additional υ Constants. *J. Org. Chem.* **1976**, *41*, 2217.

(37) Elewady, Y. A.; El-Nahas, M.; Moussa, M. N. H. Kinetics of Esterification of Some Organic Acids with Ethanol Using Amberlite IR-20 as Catalyst. *Indian J. Chem.* **1986**, *26A*, 63.

(38) Liu, Y.; Lotero, E.; Goodwin, J. G., Jr. Effect of Carbon Chain Length on Esterification of Carboxylic Acids with Methanol using Acid Catalysis. *J. Catal.* **2006**, *243*, 221.

(39) López, D. E.; Goodwin, J. G., Jr.; Bruce, D. A. Kinetics for the Transesterification of Triacetin on Nafion Acid Resins. *J. Catal.* **2007**, *245*, 379.

(40) Suwannakarn, K.; Lotero, E.; Goodwin, J. G., Jr. Solid Brønsted Acid Catalysis in the Gas Phase Esterification of Acetic Acid. *Ind. Eng. Chem. Res.* **2007**, *46*, 7050.

(41) Wachs, I. E.; Kim, T.; Ross, E. I. Catalysis Science of the Solid Acidity of Model Supported Tungsten Oxide Catalysts. *Catal. Today* **2006**, *116*, 162.

(42) Beers, A. E. W.; Spruijt, R. A.; Nijhuis, T. A.; Kapteijn, F.; Moulijn, J. A. Esterification in a Structured Catalytic Reactor with Counter-Current Water Removal. *Catal. Today* **2001**, *66*, 175.

(43) Liu, K.-S. Preparation of Fatty-Acid Methyl Esters for Gas-Chromatographic Analysis of Lipids in Biological-Materials. *J. Am Oil Chem. Soc.* **1994**, *71*, 1179.

(44) Agreda, V. H.; Partin, L. R.; William, H. H. High Purity Methyl Acetate via Reactive Distillation. *Chem. Eng. Prog.* **1990**, *86*, 40.

(45) Xu, Z. P.; Chuang, K. T. Effect of Internal Diffusion on Heterogeneous Catalytic Esterification of Acetic Acid. *Chem. Eng. Sci.* **1997**, *52*, 3011.

(46) Baertsch, C. D.; Komala, K. T.; Chua, Y.-H.; Iglesia, E. Genesis of Brønsted Acid Sites during Dehydration of 2-Butanol on Tungsten Oxide Catalysts. *J. Catal.* **2002**, *205*, 44.

Received for review May 10, 2007
Revised manuscript received January 14, 2008
Accepted January 21, 2008

IE070665A